ROCK-FABRIC/PETROPHYSICAL CLASSIFICATION OF CARBONATE PORE SPACE FOR RESERVOIR CHARACTERIZATION

by

F. Jerry Lucia

Bureau of Economic Geology

W. L. Fisher, Director

The University of Texas at Austin

Austin, Texas 78713-7508

November 1993

INTRODUCTION

The goal of reservoir characterization is to describe the spatial distribution of petrophysical parameters such as porosity, permeability, and saturation. Wireline logs, core analyses, production data, pressure buildups, and tracer tests provide quantitative measurements of petrophysical parameters in the vicinity of the wellbore. These wellbore data must be integrated with a geologic model to display the petrophysical properties in three-dimensional space. Studies that relate rock fabric to pore-size distribution, and thus to petrophysical properties, are key to quantification of geologic models in numerical terms for input into computer simulators (fig. 1).

Geologic models are generally based on observations that are interpreted in terms of depositional environments and sequences. In the subsurface, cores and wireline logs are the main source of data for these interpretations. Engineering models are based on wireline log calculations and average rock properties from core analyses. Numerical engineering data and interpretive geologic data are joined at the rock fabric level because the pore structure is fundamental to petrophysical properties and the pore structure is the result of spatially distributed depositional and diagenetic processes.

The purpose of this report is to (1) describe the relationship between carbonate rock fabrics and petrophysical properties, (2) suggest a generic petrophysical classification of carbonate pore space, and (3) determine the important geologic parameters to be mapped to allow accurate quantification of carbonate geologic models.

PORE SPACE TERMINOLOGY AND CLASSIFICATION

Pore space must be defined and classified in terms of rock fabrics and petrophysical properties in order to integrate geological and engineering information. Archie (1952) made the first attempt at relating rock fabrics to petrophysical rock properties in carbonate rocks.

The Archie classification focuses on estimating porosity but is also useful for approximating permeability and capillary properties. Archie (1952) recognized that not all the pore space can be observed using a 10-power microscope and that the surface texture of the broken rock reflected the amount of matrix porosity. Therefore, pore space is divided into matrix and visible porosity (fig. 2). *Chalky texture* is associated with a matrix porosity of about 15 percent, *sucrosic texture* indicates a matrix porosity of about 7 percent, and *compact texture* indicates matrix porosity of about 2 percent. Visible pore space is described based on pore size: A for no visible pore space and B, C, and D for increasing pore sizes from pinpoint to larger than cutting size. Porosity/permeability trends and capillary pressure characteristics are also related to these textures.

Whereas the Archie method is still useful for estimating petrophysical properties, it is difficult to relate these descriptions to geologic models because the descriptions cannot be defined in depositional or diagenetic terms. A principal difficulty is that no provision is made for distinguishing between visible interparticle pore space and other types of visible pore space such as moldic pores. Research on carbonate pore space (Lucia, 1983) has shown the importance of relating pore space to depositional and diagenetic fabrics and of distinguishing between interparticle (intergranular and intercrystalline) and other types of pore space. Recognition of the importance of these factors prompted modification of Archie's classification.

The petrophysical classification of carbonate porosity presented by Lucia (1983) emphasizes petrophysical aspects of carbonate pore space, as does the Archie classification, but by comparing rock fabric descriptions with laboratory measurements of porosity, permeability, capillarity, and Archie m values, Lucia (1983) showed that the most useful division of pore types was between pore space located between grains or crystals, called interparticle porosity, and all other pore space, called vuggy porosity (fig. 2). Vuggy pore space is further subdivided by Lucia (1983) into two groups based on how the vugs are interconnected: (1) vugs that are interconnected only through the interparticle pore network are termed *separate vugs* and (2) vugs that form an interconnected pore system are termed *touching vugs*.

Choquette and Pray (1970) discuss the geologic concepts surrounding carbonate pore space and present a classification that is widely used. They emphasize the importance of pore space genesis, and the divisions in their classification are genetic and not petrophysical. They divide all carbonate pore space into two classes: fabric selective and nonfabric selective (fig. 2). Moldic and intraparticle pore types are classified as fabric selective porosity by Choquette and Pray (1970) and grouped with interparticle and intercrystalline porosity. However, Lucia (1983) demonstrates that moldic and intraparticle pores have a different effect on petrophysical properties than do interparticle and intercrystalline pores and thus should be grouped separately. Pore-type terms used in this classification are listed in figure 3 and compared with those suggested by Choquette and Pray. Whereas most of the terms defined by Choquette and Pray are also used here, interparticle and vug porosity have different definitions. Lucia (1983) demonstrated that pore spaces located both between grains (intergranular porosity) and between crystals (intercrystalline porosity) are petrophysically similar, and a term is needed to identify these petrophysically similar pore types. The term "interparticle" was selected because of its broad connotation. The classification of Choquette and Pray (1970) does not have a term that encompasses these two petrophysically similar pore types. In their classification, the term "interparticle" is used instead of "intergranular."

Vuggy porosity, as defined by Lucia, is pore space significantly larger than or within rock particles; that is, pore space that is not interparticle. Vugs are commonly present as leached grains, fossil chambers, fractures, and large irregular cavities. This definition deviates from the restrictive definition of vugs used by Choquette and Pray (1970) as nonfabric selective pores, but it is consistant with the Archie terminology and with the widespread use in the oil industry of the term "vuggy porosity" to refer to visible pore space in carbonate rocks.

ROCK FABRIC/PETROPHYSICAL CLASSIFICATION

At the foundation of the Lucia and the Archie classifications are the concepts that pore-size distribution controls permeability and saturation and that pore-size distribution is related to rock fabric. In order to relate carbonate rock fabrics to pore-size distribution, it is important to determine if the pore space belongs to one of the three major pore-type classes, interparticle, separate-vug, or touching-vug. Each class has a different type of pore distribution and interconnection. It is equally important to determine the volume of pore space in these various classes because pore volume relates to reservoir volume and, in the case of interparticle and separate-vug porosity, to pore-size distribution.

Petrophysics of Interparticle Pore Space

In the absence of vuggy porosity, pore-size distribution in carbonate rocks can be described in terms of particle size, sorting, and interparticle porosity (fig. 4). Lucia (1983) showed that particle size can be related to mercury capillary displacement pressure in nonvuggy carbonates having more than 0.1 md permeability, suggesting that particle size describes the size of the larger pores (fig. 5). Whereas the displacement pressure characterizes the larger pore sizes, the shape of the capillary pressure curve characterizes the smaller pore sizes. Lucia (1983) suggested that the shape of the capillary pressure curve is a function of interparticle porosity and that the entry pressure is a function of particle size.

The relationship between displacement pressure and particle size (fig. 5) is hyperbolic and suggests important particle-size boundaries at 100 and 20 microns. Lucia (1983) demonstrated that three permeability fields can be defined using particle-size boundaries of 100 and 20 microns, a relationship that appears to be limited to particle sizes less than 500 microns (fig. 6).

Recent work has shown that permeability fields can be better described in geologic terms if sorting as well as particle size is considered. The approach to size and sorting used in this

petrophysical classification is similar to the grain-mud-support principle upon which Dunham's (1962) classification is built. Dunham's classification, however, is based on depositional texture, whereas petrophysical classifications are focused on contemporary rock fabrics that include depositional and diagenetic textures. Therefore, minor modifications must be made in Dunham's classification before it can be applied to a petrophysical classification.

Instead of dividing fabrics into grain support and mud support as in Dunham's classification, fabrics are divided into grain-dominated and mud-dominated (fig. 4). The important attribute of grain-dominated fabrics is the presence of open or occluded intergranular porosity and a grain-supported texture. The important attribute of mud-dominated fabrics is that the areas between the grains are filled with mud even if the grains appear to form a supporting framework.

Grainstone is clearly a grain-dominated fabric, but Dunham's packstone class bridges a boundary between large intergranular pores in grainstone and small interparticle pores in wackestones and mudstones. Some packstones have intergranular pore space, and some have the intergranular spaces filled with mud. Therefore, the packstone textural class must be divided into two rock-fabric classes, grain-dominated packstones that have intergranular pore space or cement and mud-dominated packstones that have intergranular spaces filled with mud.

Permeability/Rock-Fabric Relationships

Limestone Rock Fabrics

Examples of nonvuggy limestone petrophysical rock fabrics are illustrated in figure 7. The size of the largest pores is controlled by grain size in grainstone fabrics, whereas in mud-dominated fabrics the size of the micrite particles controls the pore-size distribution. In grain-dominated packstones, however, the pore size distribution will be controlled by pore space between grains as well as between micrite particles. Figure 8a illustrates a cross plot between air permeability and intergranular porosity for grainstones. The data are from Choquette and

Steiner's (1985) publication on the Ste. Genevieve oolite (Mississippian). The average grain size of the oolite is about 400 microns. The points on this graph are concentrated within the >100 micron permeability field.

Figure 8b illustrates a cross plot between air permeability and interparticle porosity from a Middle Eastern mud-dominated fabric containing microporosity. The data from this graph are abstracted from Moshier and others (1988). The average crystal size of the mud matrix is about 5 microns (Moshier and others, 1988). The data plot in the <20 micron permeability field.

Grain-dominated packstone is a new fabric class, and data characterizing this class are difficult to find. Lucia and Conti (1987) report on a nonvuggy grain-dominated packstone of Wolfcampian age that occurs in a core taken in Oldham County, West Texas. The grain-dominated packstone is described as a poorly sorted mixture of 150 to 300 micron grains in a matrix composed of 80-micron pellets and 10-micron calcite crystals. A porosity-permeability cross plot of these data (fig. 8c) shows that they plot on the boundary between the <20 and 20–100 micron permeability fields. An additional few data points have been gleaned from the literature, and they plot in the 100 to 20 micron permeability field.

Figure 8d illustrates a cross plot between air permeability and porosity for North Sea coccolith chalk (Scholle, 1977). The average size of the coccoliths is about 1 micron. The data points plot below the <20 micron permeability field. The presence of intrafossil pore space in the coccolith grains probably accounts for the lower than expected permeability values in the high porosity ranges.

Figure 9 illustrates all the data for limestones compared with the permeability fields. Whereas there is considerable scatter in the data, grainstone, grain-dominated packstone, and mud-dominated fabrics are reasonably well constrained to the three permeability fields. Whereas the fabrics of grain size and sorting define the permeability fields, the interparticle porosity defines the permeability within the field. Systematic changes in intergranular porosity by cementation, compaction, and dissolution processes will produce systematic changes in the

pore size distribution. Therefore, the permeability field is defined by interparticle porosity, grain size, and sorting.

Dolomite Rock Fabrics

Examples of dolomite petrophysical rock fabrics are illustrated in figures 10 and 11. Dolomitization can change the rock fabric significantly. In limestones, the grain/mud fabrics can usually be distinguished with little difficulty. If the rock has been dolomitized, however, the overprint of dolomite crystals often obscures the grain/mud fabric. Grain/mud fabrics in fine-crystalline dolostones are easily recognizable. However, as the crystal size increases, the precursor fabrics become more difficult to determine.

Dolomite crystals (defined as particles in this classification) commonly range in size from several microns to over 200 microns. Micrite particles are usually <20 microns in size. Thus, dolomitization of a mud-dominated carbonate fabric can result in an increase in particle size from <20 microns to 200 microns (fig. 11). The cross plot of interparticle-porosity and permeability (fig. 12a) illustrates the principle that, in mud-dominated fabrics, permeability increases as dolomite crystal size increases. Finely crystalline (average 15 microns) mud-dominated dolostones from Farmer and Taylor Link fields in the Permian Basin and from Choquette and Steiner (1985) plot within the <20 micron permeability field. Medium crystalline (average 50 microns) mud-dominated dolostones from Dune field, Permian Basin, (Bebout and others, 1987) plot within the 100 to 20 micron permeability field. Large crystalline (average 150 microns) mud-dominated dolostone from Andrews South Devonian field, Permian Basin (Lucia, 1962), plot in the >100 micron permeability field.

Grainstones are usually composed of grains much larger than the dolomite crystal size (fig. 10) so that dolomitization does not have a significant effect on the pore size distribution. This principle is illustrated in figure 12b, where interparticle porosity and permeability measurements from dolomitized grainstones are crossplotted. The grain size of the

dolograinstones is 200 microns. The finely crystalline dolograinstone from Taylor Link field, Permian Basin, the medium crystalline dolograinstone from Dune field, Permian Basin, and the large crystalline dolograinstone from an outcrop on the Algerita Escarpment, New Mexico, all plot within the >100 micron permeability field. The large crystalline mud-dominated fabrics also plot in this permeability field, indicating that they are petrophysically similar to grainstones (fig. 12a).

Interparticle porosity and permeability measurements from fine to medium crystalline grain-dominated dolopackstones are crossplotted in figure 12c. The samples are from Seminole San Andres Unit and Dune (Grayburg) field (Bebout and others, 1987), Permian Basin. The data plot in the 100 to 20 micron permeability field. The medium crystalline mud-dominated dolostones also plot in this field (fig. 12a).

Figure 13 illustrates all dolomite data compared with the permeability fields. Dolograinstones and large crystal dolostones constitute the >100 micron permeability field. Grains are very difficult to recognize in dolostones with >100 micron crystal size. However, since all large crystalline dolostones and all grainstones are petrophysically similar, it makes little difference petrophysically whether the crystal size or the grain size is described. Fine and medium crystalline grain-dominated dolopackstones and medium crystalline mud-dominated dolostone fabrics constitute the 100 to 20 micron permeability field. Fine crystalline mud-dominated dolostone fabrics constitute the <20 micron field.

The dolostone permeability fields are defined by dolomite crystal size as well as grain size and sorting of the precursor limestone. Within the field, permeability is defined by interparticle porosity. Systematic changes in intergranular and intercrystalline porosity by predolomite calcite cementation, dolomite cementation, and compaction will systematically change the pore size distribution. Therefore, interparticle porosity defines the permeability whereas dolomite crystal size and grain size and sorting define the permeability field.

Limestone and Dolomite Comparison

The limestone and dolostone rock fabrics that constitute the permeability fields are combined in figure 14. The fabrics that make up the >100 micron permeability field are (1) limestone and dolomitized grainstones and (2) large crystalline grain-dominated dolopackstones and mud-dominated dolostone fabrics. The effect of grain size in this field can be seen by comparing figures 9 and 13. Ooid grainstones, which have a grain size of 400 microns, are more permeable for a given porosity than dolograinstones, which have a grain size of 200 microns.

Fabrics that make up the 100 to 20 micron field are (1) grain-dominated packstones, (2) fine to medium crystalline grain-dominated dolopackstones, and (3) medium crystalline mud-dominated dolostone fabrics. A comparison of figures 11 and 16 shows that dolomitized grain-dominated packstones tend to be more permeable for a given porosity than limestone grain-dominated packstones. The <20 micron permeability field is characterized by mud-dominated limestone and fine crystalline mud-dominated dolostone fabrics.

Reduced major axis (RMA) transforms are presented below for each combined permeability field (fig. 17). The transform for the between 100 and 20 micron field is slightly skewed to the field boundaries, and a transform that is more compatible with the field boundaries is presented and recommended.

Class 1 $k = (45.35*10^{8}) * \Ø_{ip}^{8.537}$ $r = 0.71$

Class 2 $k = (1.595*10^{5}) * \Ø_{ip}^{5.184}$ $r = 0.80$

(recommended Class 2 $k = (2.040*10^{6}) * \ø_{ip}^{6.38}$)

Class 3 $k = (2.884*10^{3}) * \Ø_{ip}^{4.275}$ $r = 0.81$

where k = md, $\Ø_{ip}$ = fractional porosity

Special Types of Interparticle Porosity

Diagenesis can produce unique types of interparticle porosity. Collapse of separate-vug fabrics due to overburden pressure can produce fragments that are properly considered "diagenetic particles." Large dolomite crystals with their centers dissolved can collapse to form pockets of dolomite rim crystals. Leached grainstones can collapse to form intergranular fabrics composed of fragments of dissolved grains. These special pore types are usually not areally extensive, with the exception of collapse breccias formed by the collapse of caverns.

Capillary Pressure/Rock-Fabric Relationships

Several methods have been presented for relating porosity, permeability, water saturation, and reservoir height (Leverett, 1941; Aufricht and Koepf, 1957; Heseldin, 1974), the most recent being Alger and others (1989). These methods attempt to average the capillary pressure curves into one relationship between saturation, porosity, permeability, and reservoir height without regard to rock fabric. The data presented above demonstrate that the three nonvuggy rock-fabric fields have unique porosity-permeability relationships, suggesting that capillary properties of nonvuggy carbonates should also be separated in rock fabric categories.

To characterize the capillary properties of the three rock-fabric fields, capillary pressure curves with different interparticle porosities from the three rock-fabric fields are compared. Two curves representative of Class 1 are presented in figure 15a. Both curves are from samples of fine to medium crystalline dolograinstones. The 9.2 percent porosity curve represents the average of two sets of capillary pressure data from dolograinstones in Taylor Link field, and the 17.6 percent porosity curve represents the average of two data sets, one from the Taylor Link field and one from Dune field. Three curves representative of class 3 are presented in figure 15b. The curves are from samples of fine crystalline dolowackestones and from Farmer field. Three curves representative of class 2 are presented in figure 15c. Class 2 represents a very diverse class of rock fabrics, and it is difficult to combine all the fabrics into a few simple

curves. The curves presented here are from medium crystalline dolowackestones of the Seminole San Andres Unit and may not be representative of all grain-dominated packstones.

Each group of curves is characterized by similar displacement pressures and a systematic change in curve shape and saturation characteristics with changes in interparticle porosity. The relationship between porosity, saturation, and rock fabric class can be demonstrated by selecting a reservoir height of 500 ft (equates to a mercury capillary pressure of about 650 psia) and plotting saturation against porosity for each rock-fabric class. The results (fig. 16) show that, in nonvuggy carbonate reservoirs, a plot of porosity versus water saturation can separate the three rock-fabric groups into saturation fields similar to permeability fields.

Equations relating water saturation to porosity and reservoir height are developed in two steps. First, mercury capillary pressure is converted to reservoir height using generic values (table 1). Second, wetting-phase saturations from the capillary pressure curves are plotted against porosity for several reservoir heights. Third, lines of equal reservoir height are drawn assuming equal slopes, and a relationship between intercepts and reservoir height is developed. This relationship is substituted for the intercept term in the porosity vs. saturation equation resulting in a relationship among water saturation, porosity, and reservoir height.

The resulting equations are listed below, and three dimensional representations for classes 1 and 3 are presented in figure 17. These equations are specific to the capillary pressure curves used in this report and will not necessarily apply to specific reservoirs. However, the equations will provide reasonable values for original water saturations when porosity and rock fabric data are all that is available.

$$\text{Class 1 } Sw = 0.02219 * H^{-0.316} * \emptyset^{-1.745}$$

$$\text{Class 2 } Sw = 0.1404 * H^{-0.407} * \emptyset^{-1.440}$$

$$\text{Class 3 } Sw = 0.6110 * H^{-0.505} * \emptyset^{-1.210}$$

where H = Height above capillary pressure = 0

$\emptyset$ = Fractional porosity

Rock-fabric/Petrophysical Classes

The three rock-fabric groups define permeability and saturation fields, and therefore the three rock-fabric groups, together with interparticle porosity and reservoir height, can be used to relate petrophysical properties to geologic observations. These rock-fabric groups are herein termed *rock-fabric/petrophysical classes* (fig. 18). The classes are described below and generic transform equations presented.

Class 1 - Grainstones, dolograinstones, and large crystalline dolostones.

Class 1 $k = (45.35*10^{8}) * \emptyset_{ip}^{8.537}$

Class 1 $Sw = 0.02219 * H^{-0.316} * \emptyset^{-1.745}$

Class 2 - Grain-dominated packstones, fine and medium crystalline grain-dominated dolo-packstones, and medium crystalline mud-dominated dolostone fabrics.

Class 2 $k = (2.040*10^{6}) * \emptyset_{ip}^{6.38}$ (recommended transform)

Class 2 $Sw = 0.1404 * H^{-0.407} * \emptyset^{-1.440}$

Class 3 - Mud-dominated limestones and fine crystalline mud-dominated dolostone fabrics.

Class 3 $k = (2.884*10^{3}) *\emptyset_{ip}^{4.275}$

Class 3 $Sw = 0.6110 * H^{-0.505} *\emptyset^{-1.210}$

Petrophysics of Separate-Vug Pore Space

Separate-vug pore space is defined as pore space that is (1) either within particles or significantly larger than the particle size and (2) interconnected only through the interparticle porosity (fig. 19). Separate vugs (fig. 20) are typically fabric-selective in their origin. Intrafossil pore space, such as the living chambers of a gastropod shell; moldic pore space, such as dissolved grains (oomolds) or dolomite crystals (dolomolds); and intragranular microporosity are examples of intraparticle, fabric-selective separate vugs. Molds of evaporite crystals and fossil-molds found in mud-dominated fabrics are examples of fabric-selective separate vugs that are

significantly larger than the particle size (fig. 20). In mud-dominated fabrics, shelter pore space is typically much larger than the particle size and is classified as separate-vug porosity.

In grain-dominated fabrics, extensive selective leaching of grains may cause grain boundaries to dissolve, producing composite molds. These composite molds may have the petrophysical characteristics of separate vugs. However, if dissolution of the grain boundaries is extensive, the pore space may be interconnected well enough to be classified as solution-enlarged interparticle porosity.

Grain-dominated fabrics may contain grains with intragranular microporosity (Pittman, 1971). Intragranular microporosity is classified as a type of separate vug because it is within the particles of the rock and is interconnected only through the intergranular pore network. Mud-dominated fabrics may also contain grains with microporosity, but they present no unique petrophysical condition because of the similar pore sizes between the microporosity in the mud matrix and in the grains.

The addition of separate-vug porosity to interparticle porosity increases total porosity but does not significantly increase permeability (Lucia, 1983). Figure 21a illustrates this principle in that permeability of a moldic grainstone is less than would be expected if all the total porosity were interparticle and, at constant porosity, permeability increases with decreasing separate-vug porosity (Lucia and Conti, 1987). This principle is also true for intragranular microporosity. Figure 21b is a cross plot of data from a San Andres dolograinstone from the Permian of West Texas. The cross plot shows that the permeability of the grainstone is less than would be expected if all the porosity were interparticle.

Separate vugs found within the oil column are usually considered to be saturated with oil because of their relatively large size. Results from relative permeability experiments in samples with high separate-vug porosities show low values for water saturation. Capillary pressure curves from grainstones with moldic separate vugs, however, suggest that in some instances not all the grain-molds are filled with oil. Curve A in figure 22a has 16 percent moldic porosity, 11 percent intergranular porosity, and 5 md permeability. The curve can be interpreted as showing that

most of the intergranular porosity but only about 50 percent of the moldic porosity is filled with the nonwetting phase at most reservoir conditions. A similar interpretation can be applied to curve B. The curves could also result from not allowing the experiment to come to equilibrium.

Intragranular microporosity may contain capillary-held water leading to anomalously high water saturations within a productive interval (Pittman, 1971). The capillary characteristics of a grainstone composed of grains containing microporosity between 2 micron crystals (Keith and Pittman, 1983) and a San Andres dolograinstone with grains containing microporosity between 10 micron dolomite crystals are shown in figures 22b and 22c and illustrate that water saturations in grainstones with intragranular microporosity are significantly higher than would be expected if no intragranular microporosity were present.

Petrophysics of Touching-Vug Pore Space

Touching-vug pore systems are defined as pore space that (1) is either within the particles or significantly larger than the particle size and (2) forms an interconnected pore system of significant extent (fig. 23). Touching vugs are typically nonfabric selective in origin. Cavernous, breccia, fracture, and solution-enlarged fracture pore types commonly form an interconnected pore system on a reservoir scale and are typical touching-vug pore types (fig. 23). Fenestral pore space is commonly connected on a reservoir scale and is grouped with touching vugs because the pores are normally much larger than the grain size (Major and others, 1990).

Touching vugs are usually considered to be filled with oil in the reservoirs and can increase permeability well above what would be expected from the interparticle pore system. Lucia (1983) illustrated this fact by comparing a plot of fracture permeability versus fracture porosity to the three porosity/permeability fields for interparticle porosity (fig. 24). It is apparent from this graph that permeability in touching-vug pore systems is related principally to fracture

width and is sensitive to extremely small changes in fracture porosity. There is no effective method for measuring fracture width using the rock-fabric approach.

IMPLICATIONS FOR CONSTRUCTING A GEOLOGIC MODEL

A fundamental problem in constructing a reservoir model for input into numerical fluid-flow simulators is converting geologic observations into petrophysical rock properties, namely porosity, permeability, and saturation. The rock fabrics presented here form a framework of rock types that can be most effectively converted to petrophysical parameters. Geologic models described in terms of these rock fabrics can be most readily converted into a reservoir model. In nontouching-vug reservoirs, the most important rock fabrics to describe and map are (1) grain size and sorting using the modified Dunham classification, (2) dolomite crystal size using 20 and 100 microns as size boundaries, (3) separate-vug type with special attention to intragranular microporosity, (4) total porosity, and (5) separate-vug porosity.

The stacking patterns of rock-fabric units are systematic within a depositional and diagenetic environment (Lucia, 1993). The simplest example is the upward-shoaling bar complex. Mud-dominated fabrics grade upward and laterally into grain-dominated fabrics with a corresponding increase in permeability, decrease in water saturation, and little change in porosity (fig. 25). The permeability and water saturation are a function of total porosity and rock fabric. The introduction of moldic porosity (separate vugs) by selective dissolution of grains in the grain-dominated fabric, due perhaps to shoaling and the introduction of meteoric water at a subaerial exposure surface, can produce a diagenetic overprint that results in (1) no significant change in porosity, (2) little change in water saturation assuming the molds are filled with hydrocarbons, and (3) drastically reduced permeability in the grainstone (fig. 25). The permeability will be a function of interparticle porosity determined by subtracting separate-vug porosity from total porosity.

Conversion of the upward-shoaling bar complex from limestone to 50-micron crystalline dolostone will not change the grain size and sorting characteristics of the grain-dominated fabrics but will alter the particle size characteristics of the mud-dominated fabrics. Dolomitization may reduce the total porosity of the grain-dominated fabrics, but the permeability and water saturation will still be a function of grain size, sorting, and intergranular porosity. If the precursor limestone is a moldic grain-dominated fabric, the resulting grain-dominated dolostone fabric will be moldic (fig. 25). Dolomitization of the mud-dominated fabric to a 50-micron crystalline dolostone may reduce the porosity but will increase the permeability and decrease the water saturation significantly.

These examples illustrate the importance of mapping the rock fabric units. If the upward-shoaling cycle is mapped as a bar facies, the permeability and saturation structure are compromised and the resulting model is oversimplified. However, geostistical studies have suggested that the petrophysical properties within a rock-fabric unit are near randomly distributed and thus can be legitimately averaged (Lucia and others, 1992; Senger and others, 1993). If the diagenetic facies are not included as mapping parameters, the permeability and saturation values in the resulting reservoir model could be in serious error. Permeability can be significantly overestimated if the estimate is based on total porosity rather than total porosity less separate-vug porosity. If the effects of dolomitization are not included in the model, extrapolations of permeability and saturation can be seriously underestimated.

SUMMARY

The goal of reservoir characterization is to describe the spatial distribution of petrophysical parameters such as porosity, permeability, and saturation. The rock-fabric approach presented here is based on the premise that pore-size distribution controls the engineering parameters of permeability and saturation and that pore-size distribution is related to rock fabric, a product of

geologic processes. Thus, rock fabric integrates geologic interpretation with engineering numerical measurements.

To determine the relationships between rock fabric and petrophysical parameters, it is necessary to define and classify pore space as it exists today in terms of petrophysical properties. This is best accomplished by dividing pore space into pore space located between grains or crystals, called interparticle porosity, and all other pore space, called vuggy porosity. Vuggy pore space is further subdivided into two groups based on how the vugs are interconnected: (1) vugs that are interconnected only through the interparticle pore network are termed *separate vugs* and (2) vugs that are in direct contact between vugs are termed *touching vugs*.

The petrophysical properties of interparticle pore space are related to particle size, sorting, and interparticle porosity. Grain size and sorting of grains and micrite are based on Dunham's (1962) classification and modified to make it compatible with petrophysical considerations. Instead of dividing fabrics into grain support and mud support, fabrics are divided into grain-dominated and mud-dominated. The important attributes of grain-dominated fabrics are the presence of open or occluded intergranular porosity and a grain-supported texture. The important attribute of mud-dominated fabrics is that the areas between the grains are filled with mud even if the grains appear to form a supporting framework.

Grainstone is clearly a grain-dominated fabric, but Dunham's packstone class bridges an important petrophysical boundary. Some packstones have intergranular pore space and some have intergranular spaces filled with mud. Therefore, the packstone textural class must be divided into two rock-fabric classes, (1) grain-dominated packstones that have intergranular pore space or cement and (2) mud-dominated packstones, in which the intergranular spaces are filled with mud.

The important fabric elements to recognize for petrophysical classification of dolomites are precursor grain size and sorting, dolomite crystal size, and intercrystalline porosity. Important dolomite crystal size boundaries are 20 and 100 microns. Dolomite crystal size has little effect

on the petrophysical properties of grain-dominated dolostone fabrics. The petrophysical properties of mud-dominated fabrics, however, are significantly improved when the dolomite crystal size is <20 microns.

Permeability and saturation characteristics of interparticle porosity can be grouped into three rock-fabric/petrophysical classes. Class 1 is composed of (a) limestone and dolomitized grainstones and (b) large crystalline grain-dominated dolopackstones and mud-dominated dolostone fabrics. Class 2 is composed of (a) grain-dominated packstones, (b) fine to medium crystalline grain-dominated dolopackstones, and (c) medium crystalline mud-dominated dolostone fabrics. Class 3 is composed of mud-dominated limestone and fine crystalline mud-dominated dolostone fabrics.

Generic permeability transforms and water saturation, porosity, reservoir-height equations for each rock-fabric/petrophysical class are presented below.

Class 1 - Grainstones, dolgrainstones, and large crystalline dolostones.

Class 1 $k = (45.35*10^{8}) * \emptyset_{ip}^{8.537}$

Class 1 $Sw = 0.02219 * H^{-0.316} * \emptyset^{-1.745}$

Class 2 - Grain-dominated packstones, fine and medium crystalline grain-dominated dolopackstones, and medium crystalline mud-dominated dolostone fabrics.

Class 2 $k = (2.040*10^{6}) * \emptyset_{ip}^{6.38}$ (recommended transform)

Class 2 $Sw = 0.1404 * H^{-0.407} * o^{-1.440}$

Class 3 - Mud-dominated limestones and fine crystalline mud-dominated dolostone fabrics.

Class 3 $k = (2.884*10^{3}) * \emptyset_{ip}^{4.275}$

Class 3 $Sw = 0.6110 * H^{-0.505} * \emptyset^{-1.210}$

The addition of separate-vug porosity to interparticle porosity increases total porosity but does not significantly increase permeability. Therefore, it is important to determine interparticle porosity by subtracting separate-vug porosity from total porosity and use interparticle porosity to estimate permeability. Separate-vug porosity is normally considered to

be filled with hydrocarbons in the reservoir. Intergranular microporosity, however, may contain significant amounts of capillary-bound water, resulting in water-free production of hydrocarbons from intervals with higher than expected water saturation.

Touching-vug pore systems cannot be related to porosity but are related principally to fracture width. Because there is no effective method for making this observation in the reservoir, the rock fabric approach cannot be used to characterize touching-vug reservoirs.

The key to constructing a geologic model that can be quantified in petrophysical terms is to select facies or units that have unique petrophysical qualities for mapping. Petrophysical properties in rock fabric facies or units are near randomly distributed and can be legitimately averaged, making these geologic units ideal for petrophysical quantification. In nontouching vug reservoirs, the most important rock fabrics to describe and map are (1) grain size and sorting using the modified Dunham classification, (2) dolomite crystal size using 20 and 100 microns as size boundaries, (3) separate-vug type with special attention to intergranular microporosity, (4) total porosity, and (5) separate-vug porosity.

In touching vug reservoirs, characterizing the pore system is difficult because the pore system is not related to a precursor depositional fabric but is usually wholly diagenetic in nature. While it may conform to bedding, as in the case of evaporite collapse brecciation, it more often cuts across stratal boundaries. However, the recognition of the presence of a touching vug pore system is paramount because it may dominate the flow characteristics of the reservoir.

REFERENCES

Alger, R. P., Luffel, D. L., and Truman, R. B., 1989, New unified method of integrating core capillary pressure data with well logs: Society of Petroleum Formation Evaluation, v. 4, no. 2, p. 145–152.

Archie, G. E., 1952, Classification of carbonate reservoir rocks and petrophysical considerations: American Association of Petroleum Geologists Bulletin, v. 36, no. 2, p. 278–298.

Aufricht, W. R., and Koepf, E. H., 1957, The interpretation of capillary pressure data from carbonate reservoirs: Transactions, AIME, v. 210, p. 402–405.

Bebout, D. G., Lucia, F. J., Hocott, C. F., Fogg, G. E., and Vander Stoep, G. W., 1987, Characterization of the Grayburg reservoir, University Lands Dune Field, Crane County, Texas: The University of Texas at Austin, Bureau of Economic Geology Report of Investigations No. 168, 98 p.

Choquette, P. W., and Pray, L. C., 1970, Geologic nomenclature and classification of porosity in sedimentary carbonates: American Association of Petroleum Geologists Bulletin, v. 54, no. 2, p. 207–250.

Choquette, P. W., and Steiner, R. P., 1985, Mississippian oolite and non-supratidal dolomite reservoirs in the Ste. Genevieve Formation, North Bridgeport Field, Illinois Basin, *in* Roehl, P. O., and Choquette, P. W., eds., Carbonate petroleum reservoirs: Springer-Verlag, p. 209–238.

Dunham, R. J., 1962, Classification of carbonate rocks according to depositional texture, *in* Classifications of carbonate rocks—a symposium: AAPG Memoir no. 1, p. 108–121.

Heseldin, G. M., 1974, A method of averaging capillary pressure curves: SPWLA Annual Logging

Symposium, June 2-5, paper E.

Keith, B. D., and Pittman, E. D., 1983, Bimodal porosity in oolitic reservoir—effect on productivity and log response, Rodessa Limestone (Lower Cretaceous), East Texas Basin: American Association of Petroleum Geologists Bulletin, v. 67, no. 9, p. 1391–1399.

Leverett, M. C., 1941, Capillary behavior in porous solids: Transactions, AIME, v. 142, p. 151–169.

Lucia, F. J., Kerans, Charles, and Senger, R. K., 1992, Defining flow units in dolomitized carbonate-ramp reservoirs: Society of Petroleum Engineers, Paper No. SPE 24702, p. 399–406.

Lucia, F. J., 1993, Carbonate reservoir models: facies, diagenesis, and flow characterization, *in* Morton-Thompson, Diana, and Woods, A. M., eds., Development geology reference manual: AAPG Methods in Exploration Series No. 10, p. 269–274.

Lucia, F. J., 1962, Diagenesis of a crinoidal sediment: Journal of Sedimentary Petrology, v. 32, no. 4, p. 848–865.

Lucia, F. J., 1983, Petrophysical parameters estimated from visual description of carbonate rocks: a field classification of carbonate pore space: Journal of Petroleum Technology, March, p. 626–637.

Lucia, F. J., and Conti, R. D., 1987, Rock fabric, permeability, and log relationships in an upward-shoaling, vuggy carbonate sequence: The University of Texas at Austin, Bureau of Economic Geology Geological Circular 87-5, 22 p.

Major, R. P., Vander Stoep, G. W., and Holtz, M. H., 1990, Delineation of unrecovered mobile oil in a mature dolomite reservoir: East Penwell San Andres Unit, University Lands, West Texas: The University of Texas at Austin Bureau of Economic Geology Report of

Investigations No. 194, 52 p.

Moshier, S. O., Handford, C. R., Scott, R. W., and Boutell, R. D., 1988, Giant gas accumulation in "chalky"-textured micritic limestones, Lower Cretaceous Shuaiba Formation, Eastern United Arab Emirates, *in* Lomando, A. J., and Harris, P. M., eds., Giant oil and gas fields, SEPM Core Workshop no. 12, v. 1, p. 229–272.

Pittman, E. D., 1971, Microporosity in carbonate rocks: American Association of Petroleum Geologists Bulletin, v. 55, no. 10, p. 1873–1881.

Scholle, P. A., 1977, Chalk diagenesis and its relation to petroleum exploration: Oil from chalks, a modern miracle?: American Association of Petroleum Geologists Bulletin, v. 61, no. 7, p. 982–1009.

Senger, R. K., Lucia, F. J., Kerans, Charles, and Ferris, M. A., 1993, Dominant control of reservoir-flow behavior in carbonate reservoirs as determined from outcrop studies, *in* Linville, Bill, Burchfield, R. E., and Wesson, T. C., eds., Reservoir characterization III: Tulsa, Oklahoma, Pennwell Books, p. 107–150.

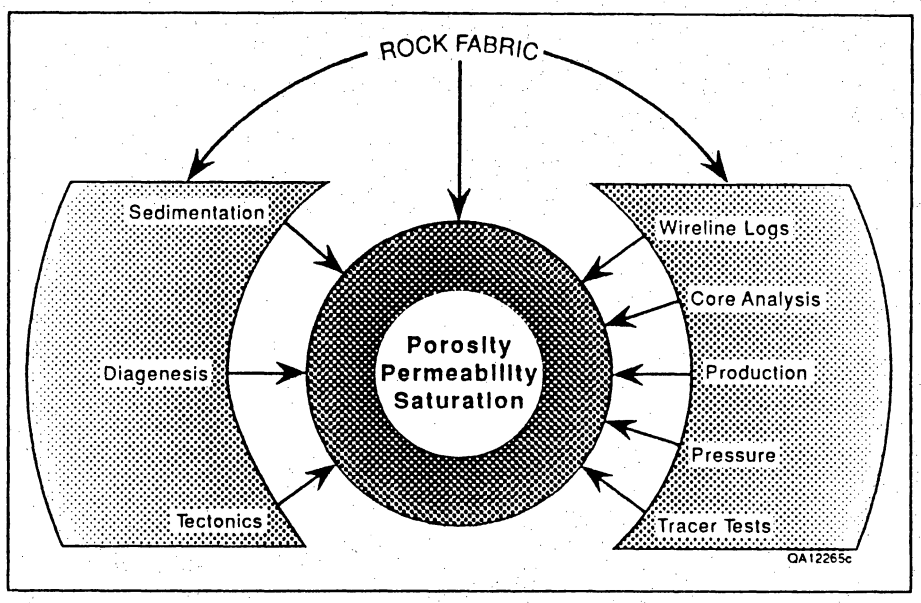

Figure 1. Integration of spatial geologic data with numerical engineering data through rock-fabric studies.

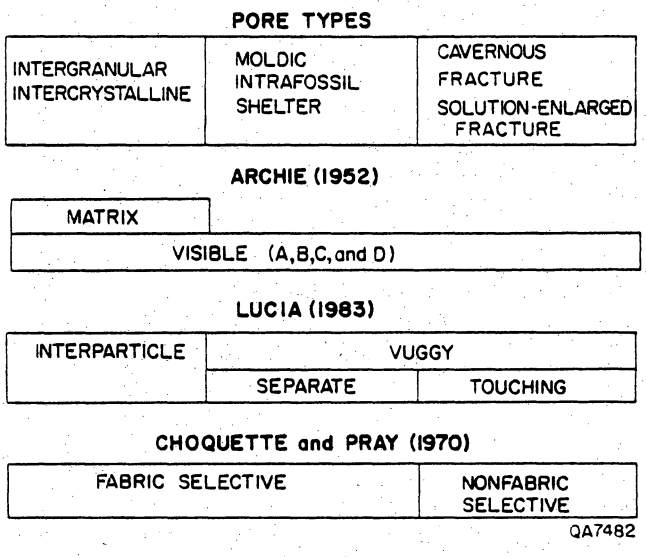

Figure 2. Petrophysical classification of carbonate pore types used in this report compared with Archie's original classification (1952) and the fabric selectivity concept of Choquette and Pray (1970).

Term	Abbreviations	
	Lucia	Choquette and Pray
Interparticle	IP	BP
Intergranular	IG	Not used
Intercrystalline	IX	BC
Vug	VUG	VUG
Separate Vug	SV	Not used
Moldic	MO	MO
Intraparticle	WP	WP
Intragranular	WG	Not used
Intracrystal	WX	Not used
Intrafossil	WF	Not used
Intragranular microporosity	μG	Not used
Shelter	SH	SH
Touching Vug	TV	Not used
Fracture	FR	FR
Solution enlarged fracture	SF	CH(channel)
Cavernous	CV	CV
Breccia	BR	BR
Fenestral	FE	FE

Figure 3. Pore type terminology used in this report compared with terminology of Choquette and Pray (1970).

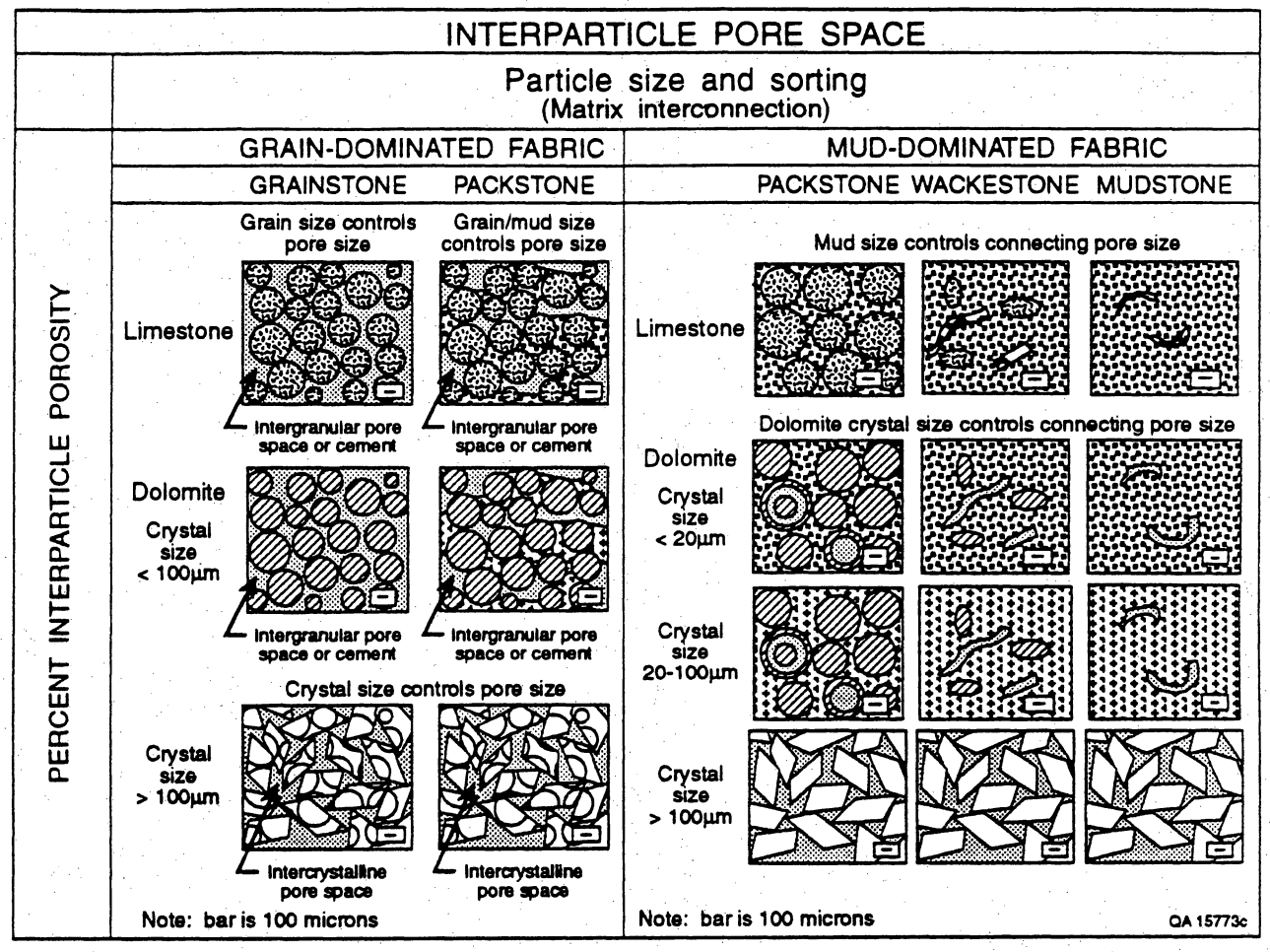

Figure 4. Geological/petrophysical classification of carbonate interparticle pore space based on size and sorting of grains and crystals.

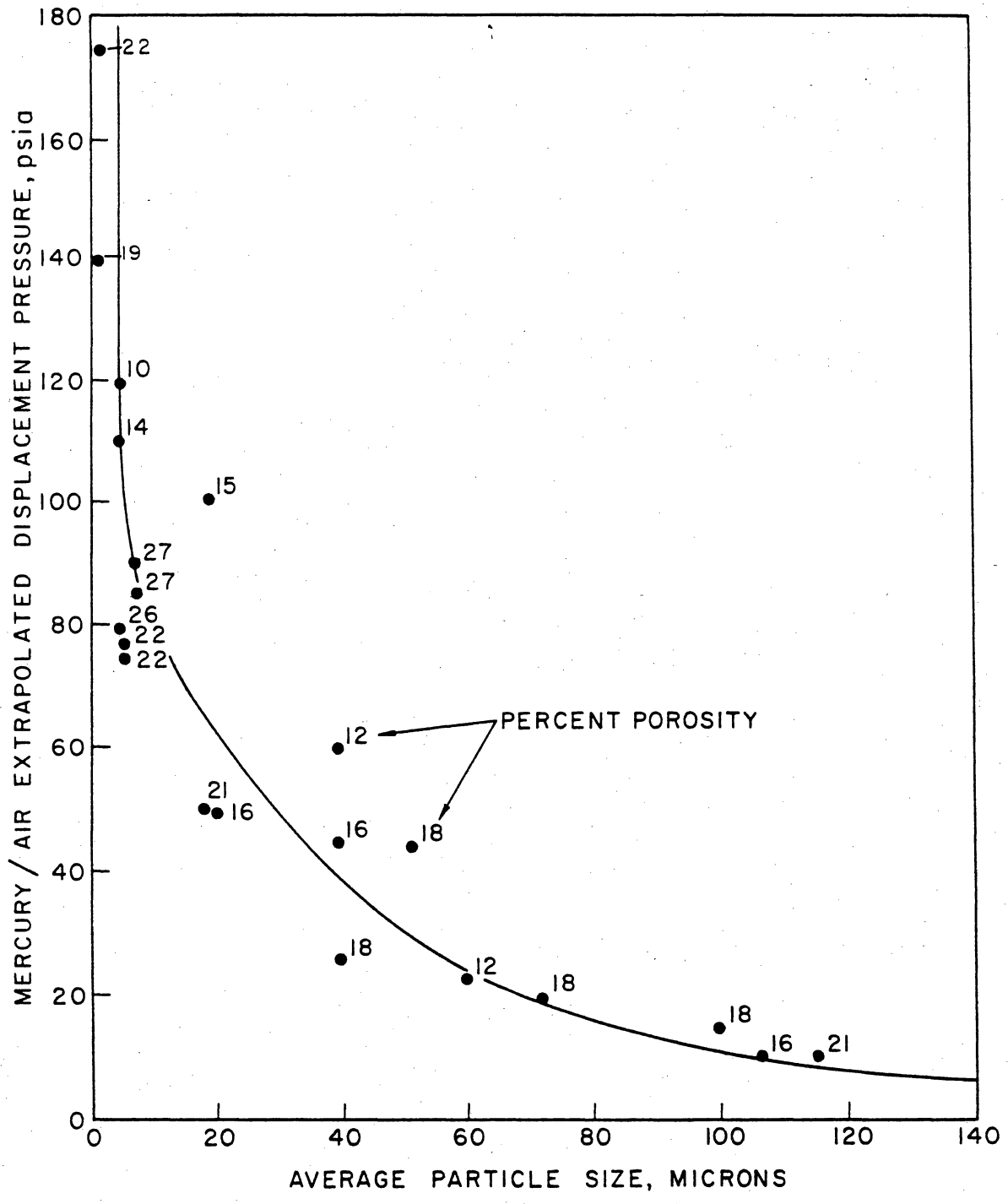

Figure 5. Relationship between Pd and average particle size for nonvuggy carbonate rocks with greater than 0.1 md (Lucia, 1983).

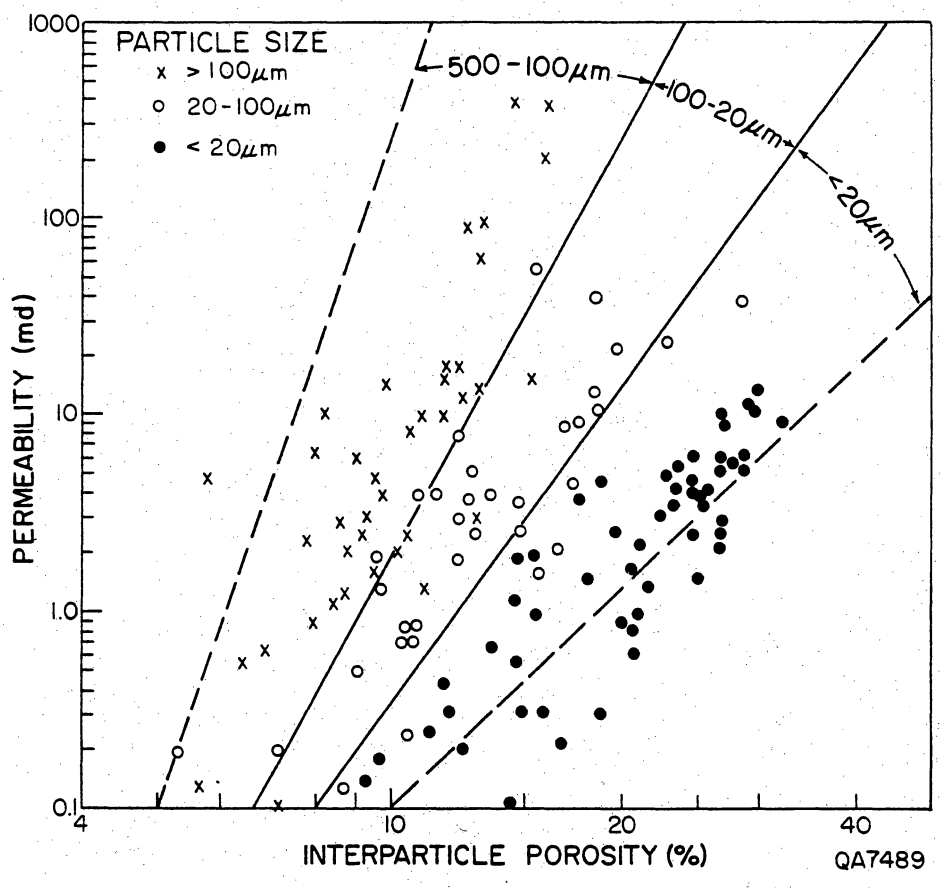

Figure 6. Porosity-permeability relationship for various particle-size groups in nonvuggy carbonate rocks (Lucia, 1983).

Figure 7. Examples of nonvuggy limestone rock fabrics. (A) Grainstone. (B) Grain-dominated packstone. Note intergranular cement and pore space. (C) Mud-dominated packstone. (D) Wackestone.

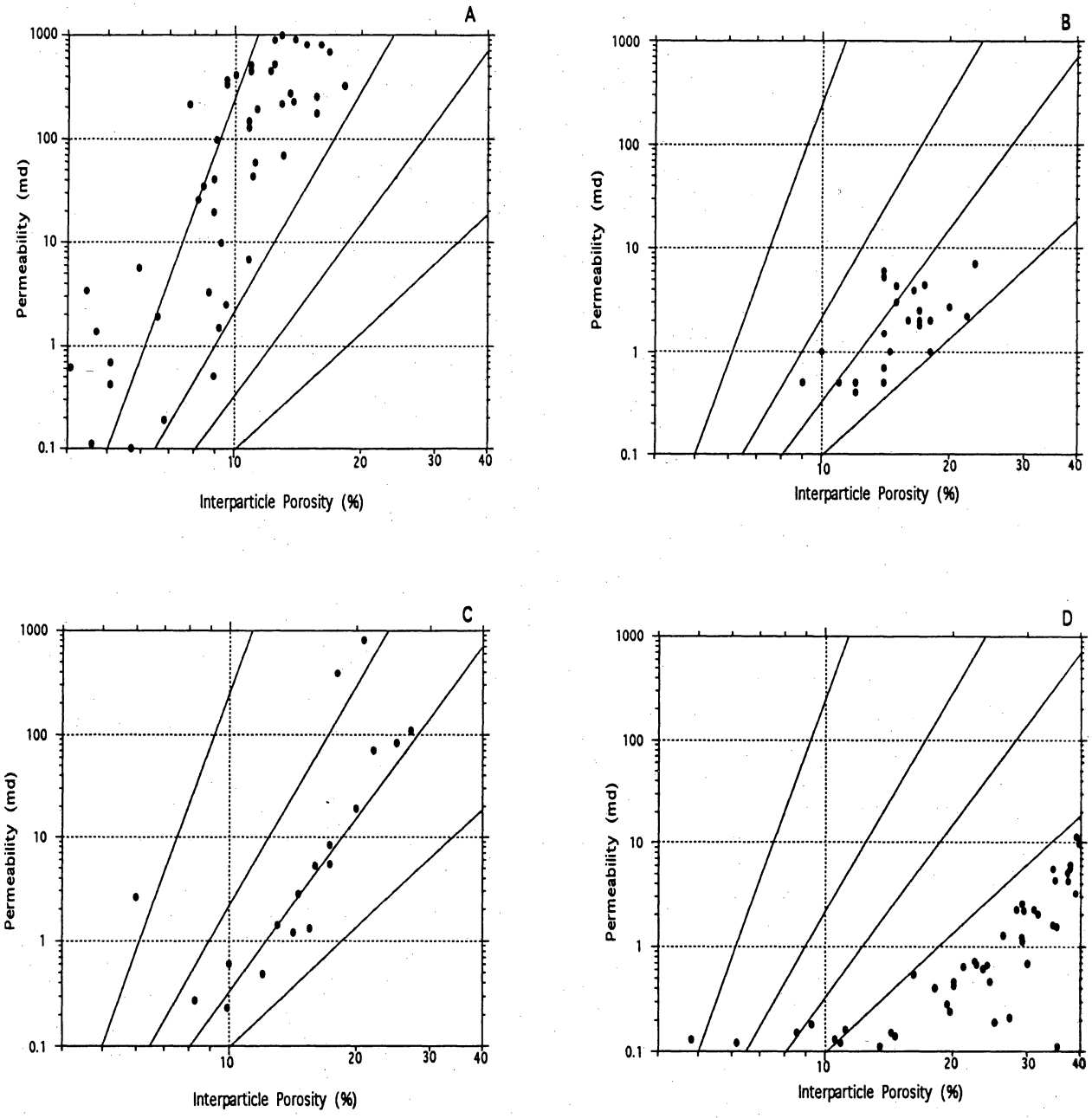

Figure 8. Porosity-permeability cross plots for nonvuggy limestone rock fabrics. (A) 400 micron oold grainstone, Ste. Genevieve (Choquette and Steiner (1985). Low-permeability, high-porosity data are deleted because they are from oomoldic and wackestone rock fabrics (personal communication from Choquette). (B) Wackestones with microporosity between 5 micron crystals from Moshier and others (1988). Data associated with stylolites not shown. (C) Grain-dominated packstone data from Lucia and Conti (1987). A poorly sorted mixture of 80 to 300 micron grains and micrite. (D) Coccolith chalk (Scholle, 1977). The presence of intragranular pore space in the coccoliths causes the data to plot below the <20 micron field.

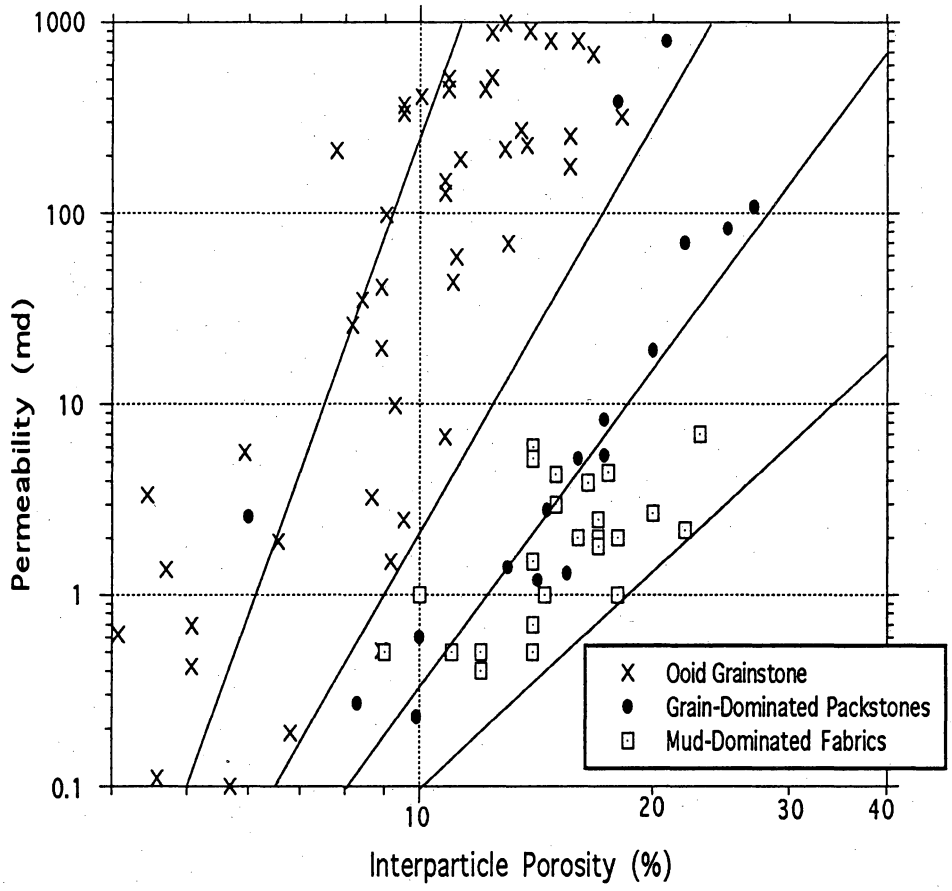

Figure 9. Composite porosity-permeability cross plot for nonvuggy limestone fabrics.

Figure 10. Examples of nonvuggy grain-dominated dolomite fabrics. (A) Dolograinstone, 15 micron dolomite crystal size. Dune field (Bebout and others, 1987). (B) Grain-dominated dolopackstone, 10 micron dolomite crystal size. Farmer field, West Texas. (C) Dolograinstone, 30 micron dolomite crystal size. Seminole San Andres Unit, West Texas. (D) Grain-dominated dolopackstone, 30 micron dolomite crystal size. Seminole San Andres Unit, West Texas. (E) Dolograinstone, crystal size 400 microns. Harmatton field, Alberta, Canada.

Figure 11. Examples of nonvuggy mid-dominated dolomite fabrics. (A) Fine crystalline dolowackestone, 10 micron dolomite crystal size. Devonian, North Dakota. (B) Medium crystalline dolowackestone, 80 micron dolomite crystal size. Devonian North Dakota. (C) Large crystalline dolowackestone, 150 micron dolomite crystal size. Andrews South Devonian field, West Texas.

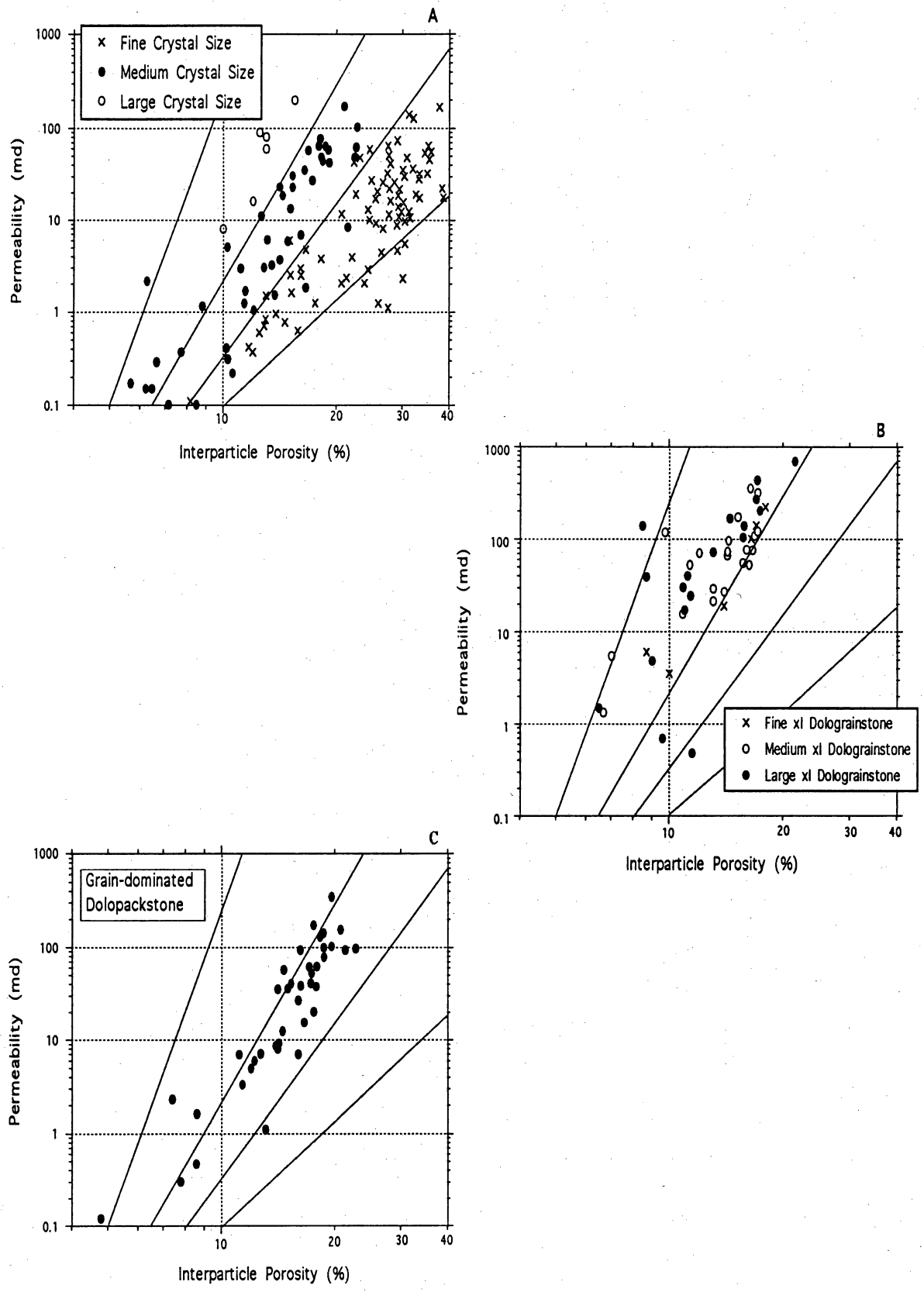

Figure 12. Porosity-permeability cross plots of nonvuggy dolomite fabrics. (A) Mud-dominated dolostone fabrics with varying dolomite crystals sizes from 10 to 150 microns. (B) Dolograinstones (average grain size is 200 microns) with varying dolomite crystal sizes from 15 to 150 microns. (C) Grain-dominated dolopackstones with fine to medium dolomite crystal sizes.

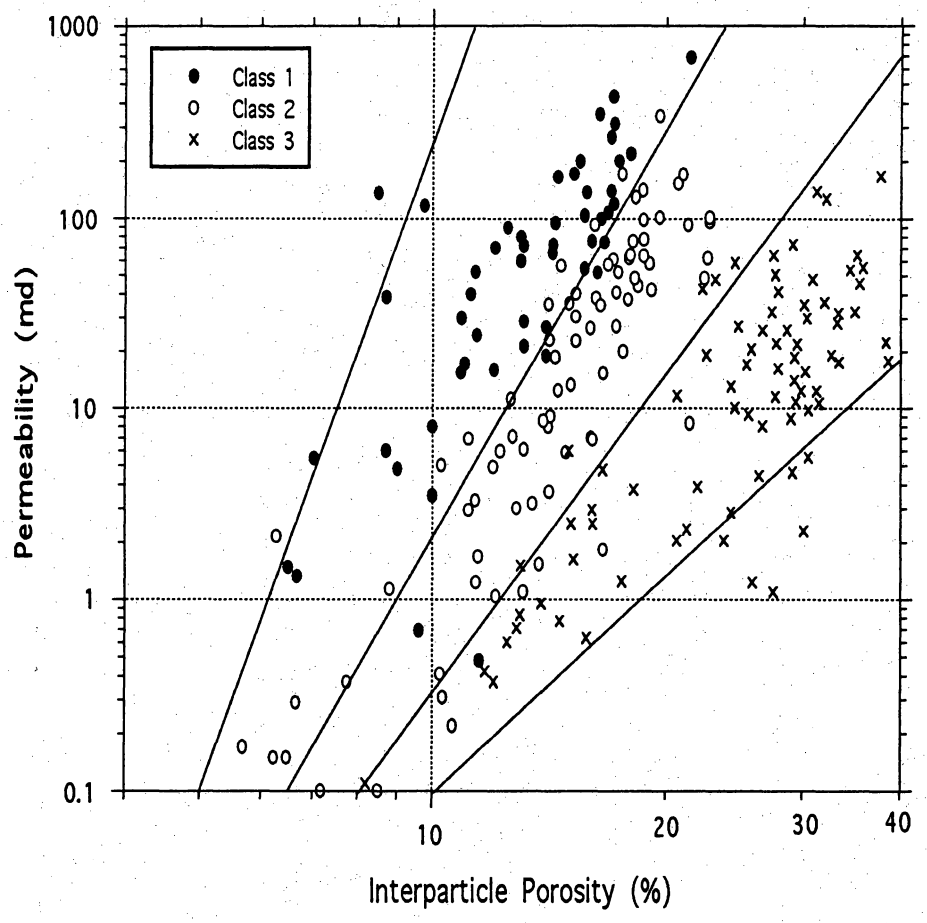

Figure 13. Composite porosity-permeability cross plot for nonvuggy dolostone fabrics.

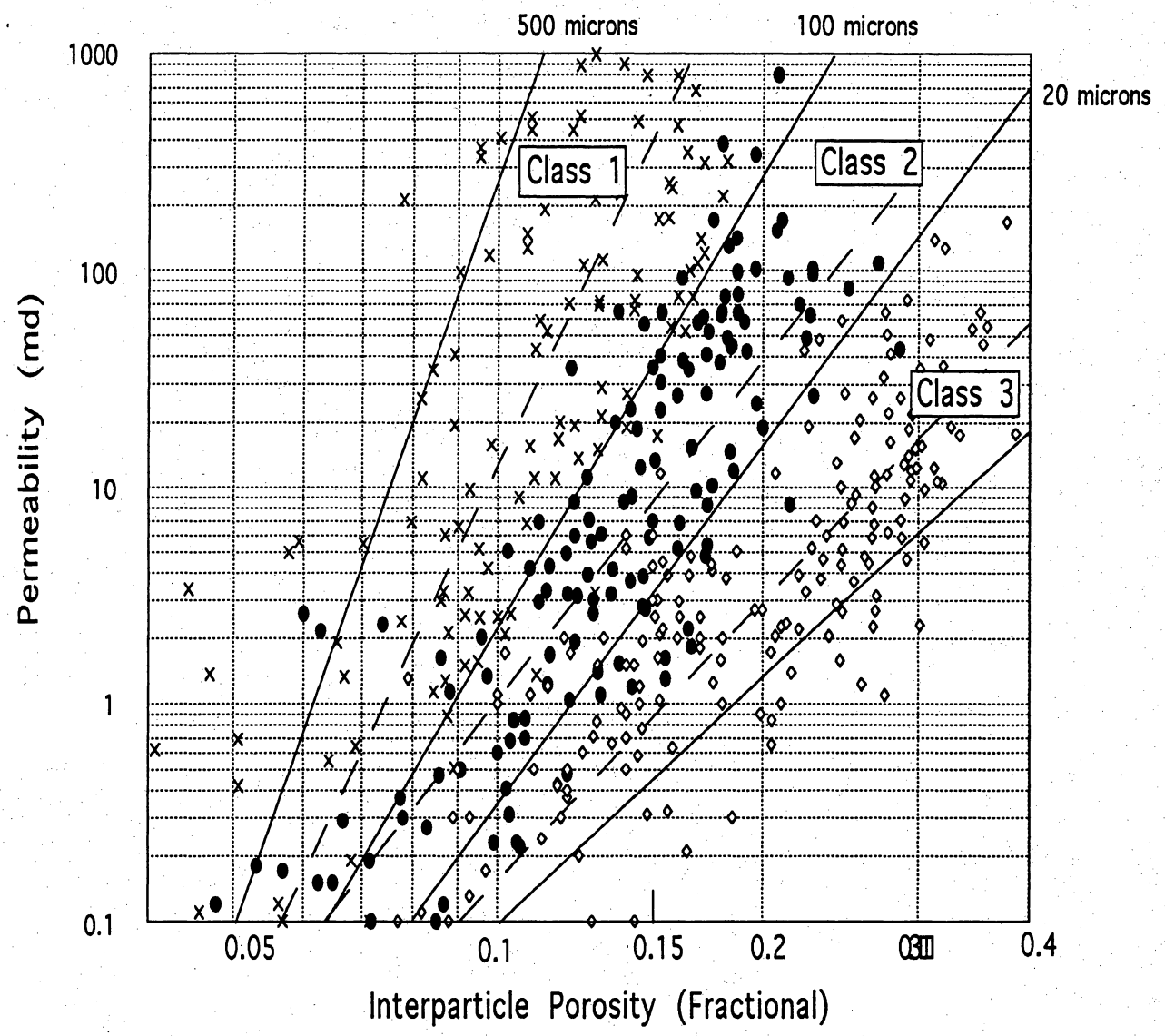

Figure 14. Composite porosity-permeability cross plot for nonvuggy limestones and dolostones showing statistical reduced major axis transforms for each class.

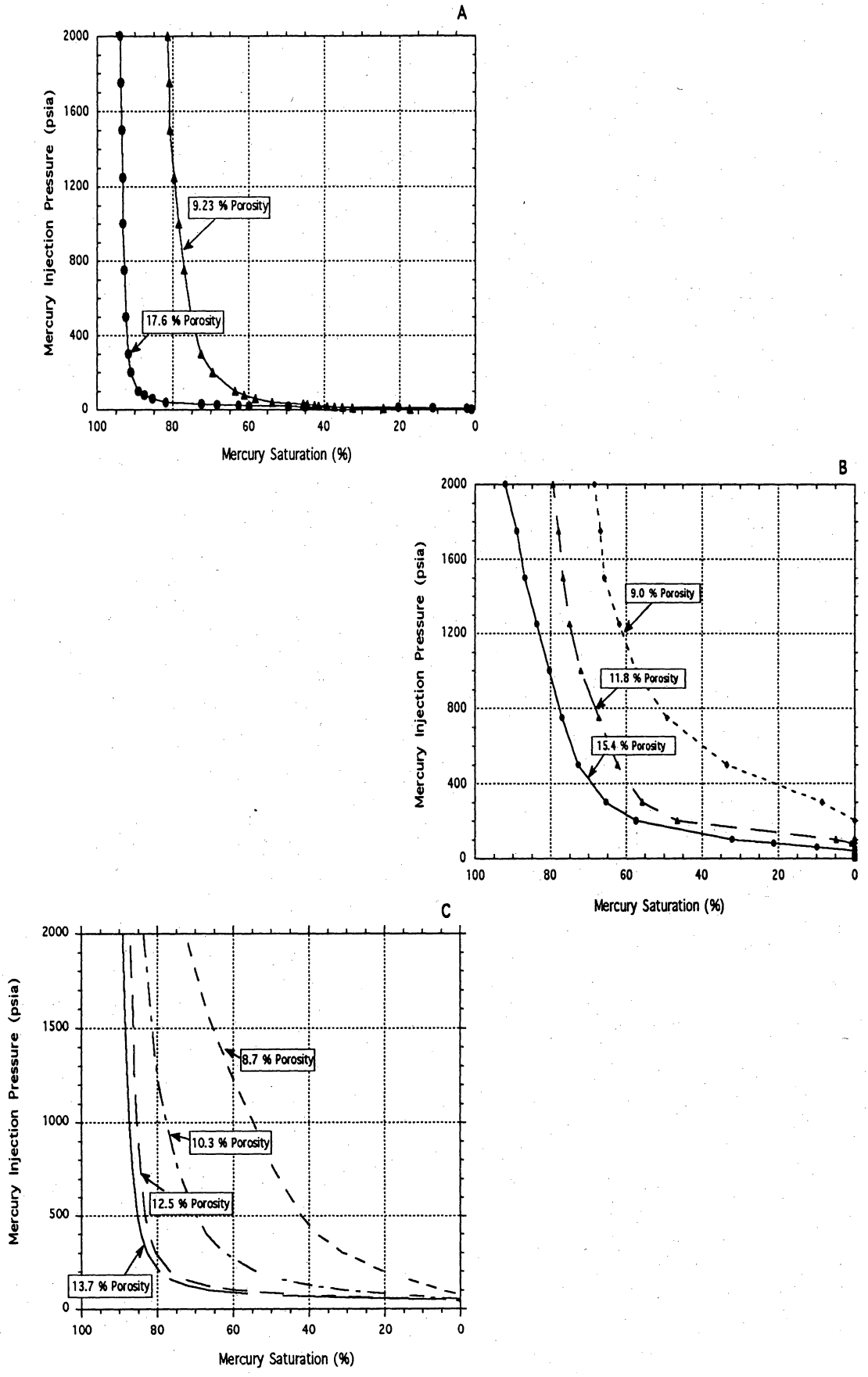

Figure 15. Capillary pressure curves for petrophysical classes. (A) Class 1. Data presented are from dolograinstones. (B) Class 3. Data presented are from fine crystalline dolowackestones. C) Class 2. Data are from medium crystalline dolowackestones.

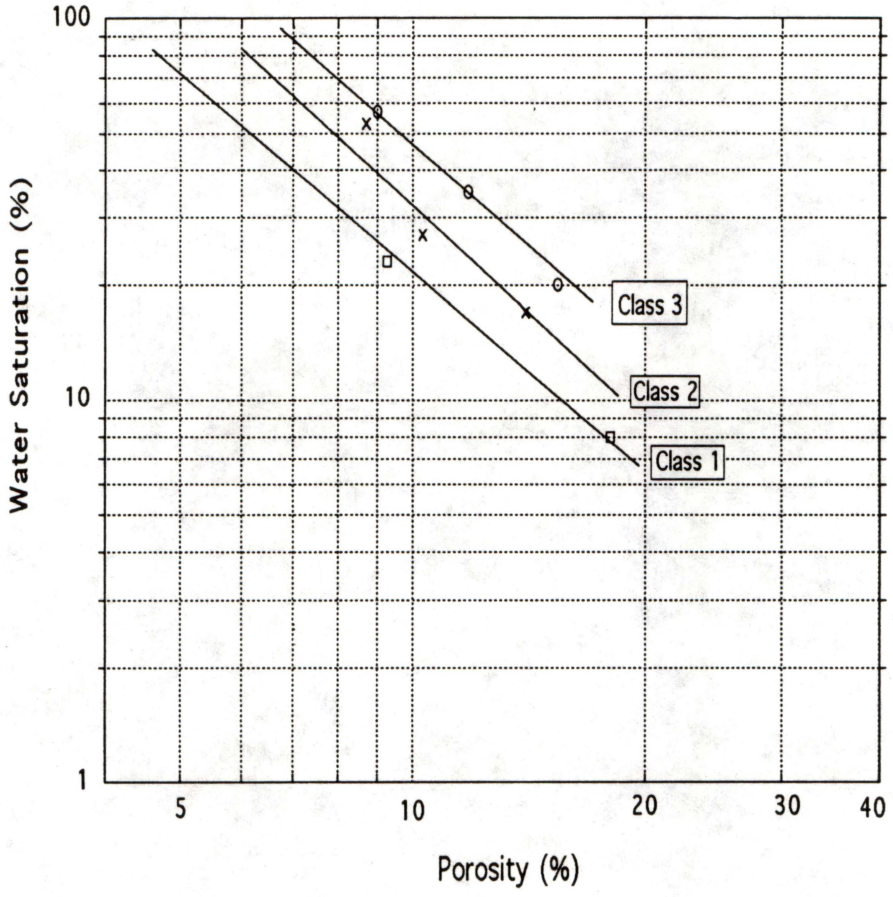

Figure 16. Cross plot of porosity and water saturation for the three rock-fabric petrophysical classes at a reservoir height of 500 ft. Water saturation and porosity values are taken from capillary pressure curves illustrated in figure 15.

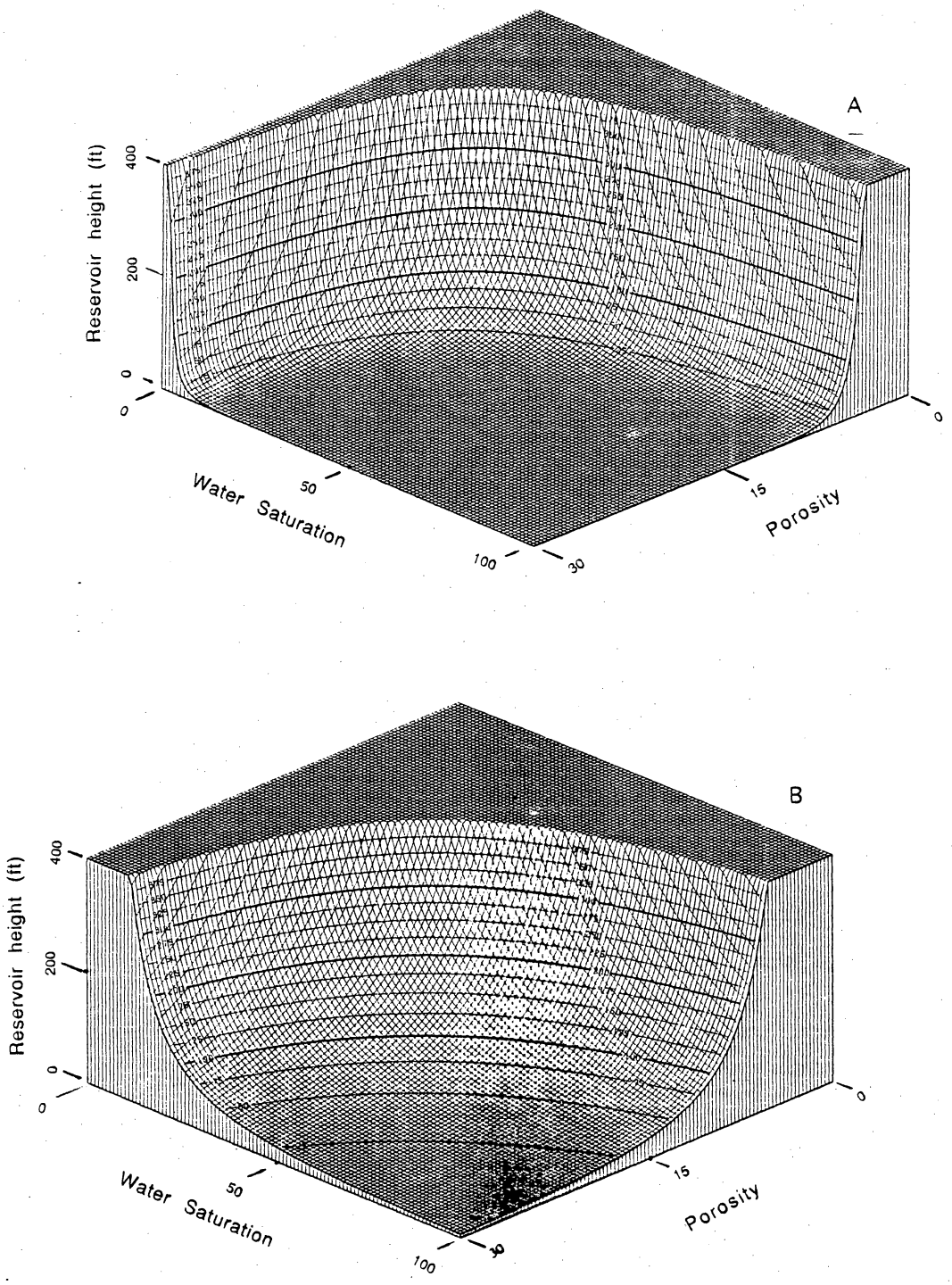

Figure 17. Three-dimensional displays of class 1 and class 3 equations relating water saturation to reservoir height and porosity. (A) Class 1 curve. (B) Class 3 curve.

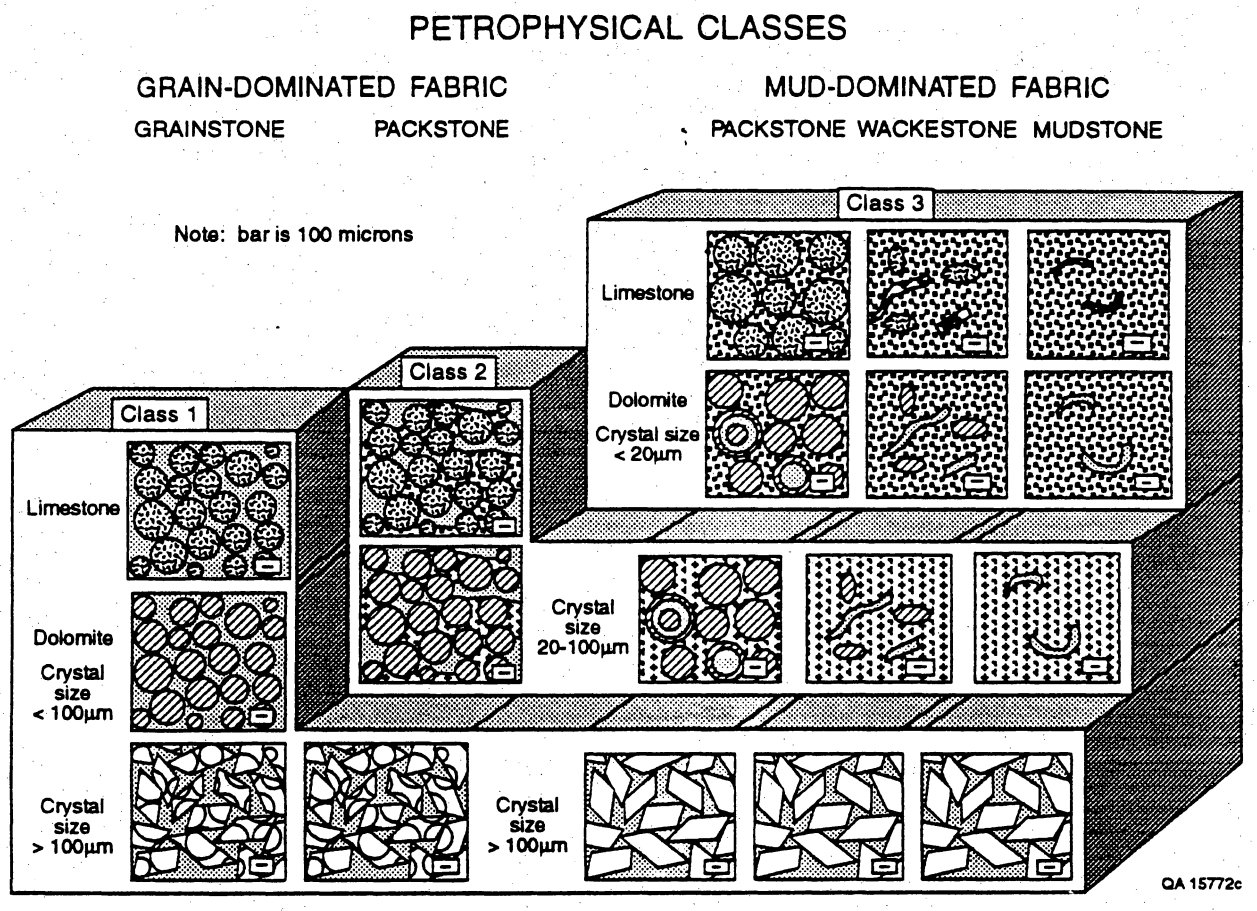

Figure 18. Petrophysical/rock-fabric classes based on similar capillary properties and interparticle-porosity/permeability transforms.

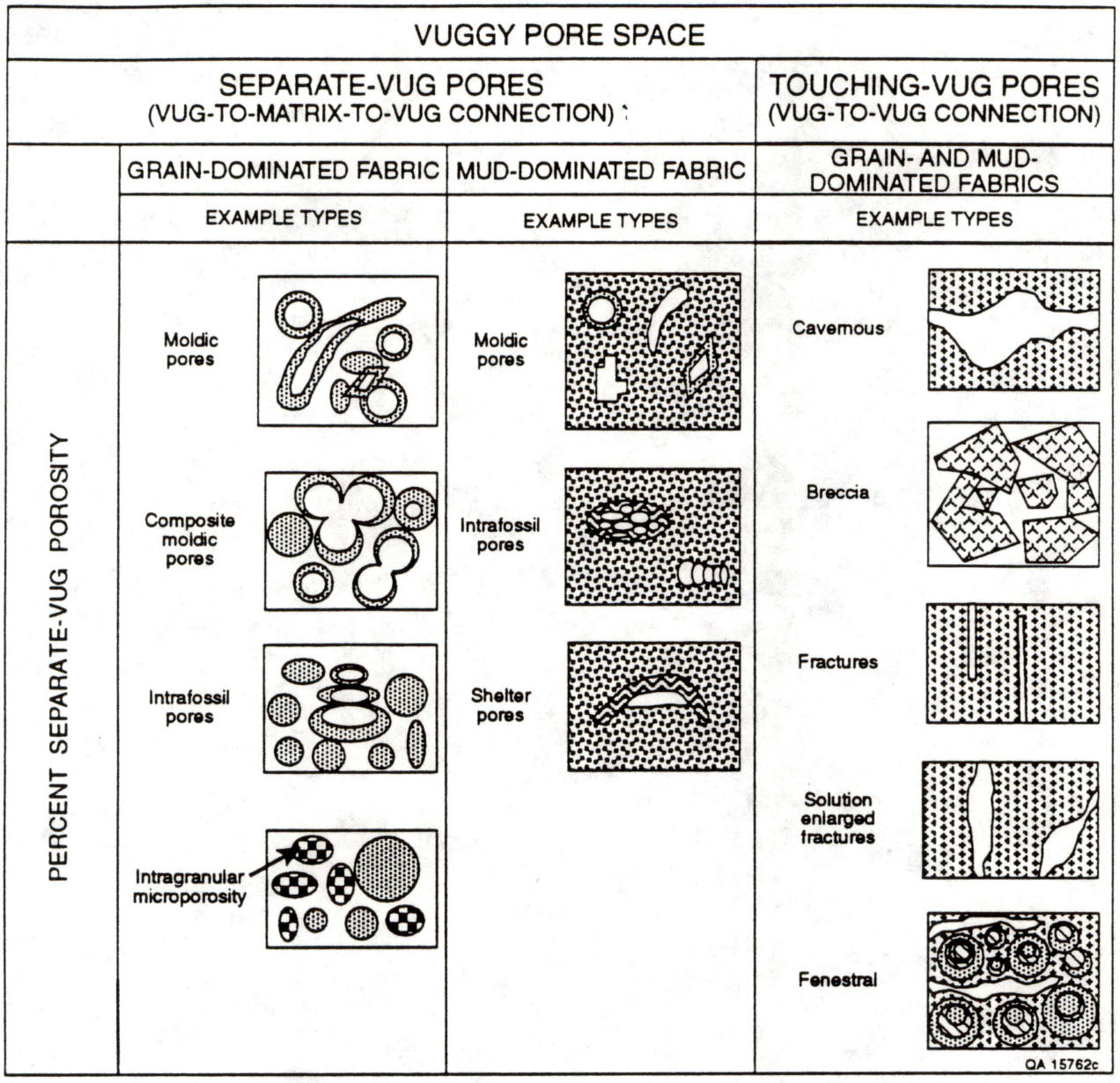

Figure 19. Geological/petrophysical classification of vuggy pore spaces based on vug interconnection.

Figure 20. Examples of separate vug pore types. (A) Oomoldic porosity, Wolfcampian, West Texas. (B) Intrafossil pore space in a gastropod shell, Cretaceous, Gulf Coast. (C) Fossil molds in wackestone. (D) Anhydrite molds in grain-dominated packstone, Mississippian, Montana. (E) Fine crystalline dolograinstone with intragranular microporosity, Farmer field, West Texas. (F) Scanning electron photomicrograph of dolograins in (E) showing intragranular microporosity between 10 micron crystals.

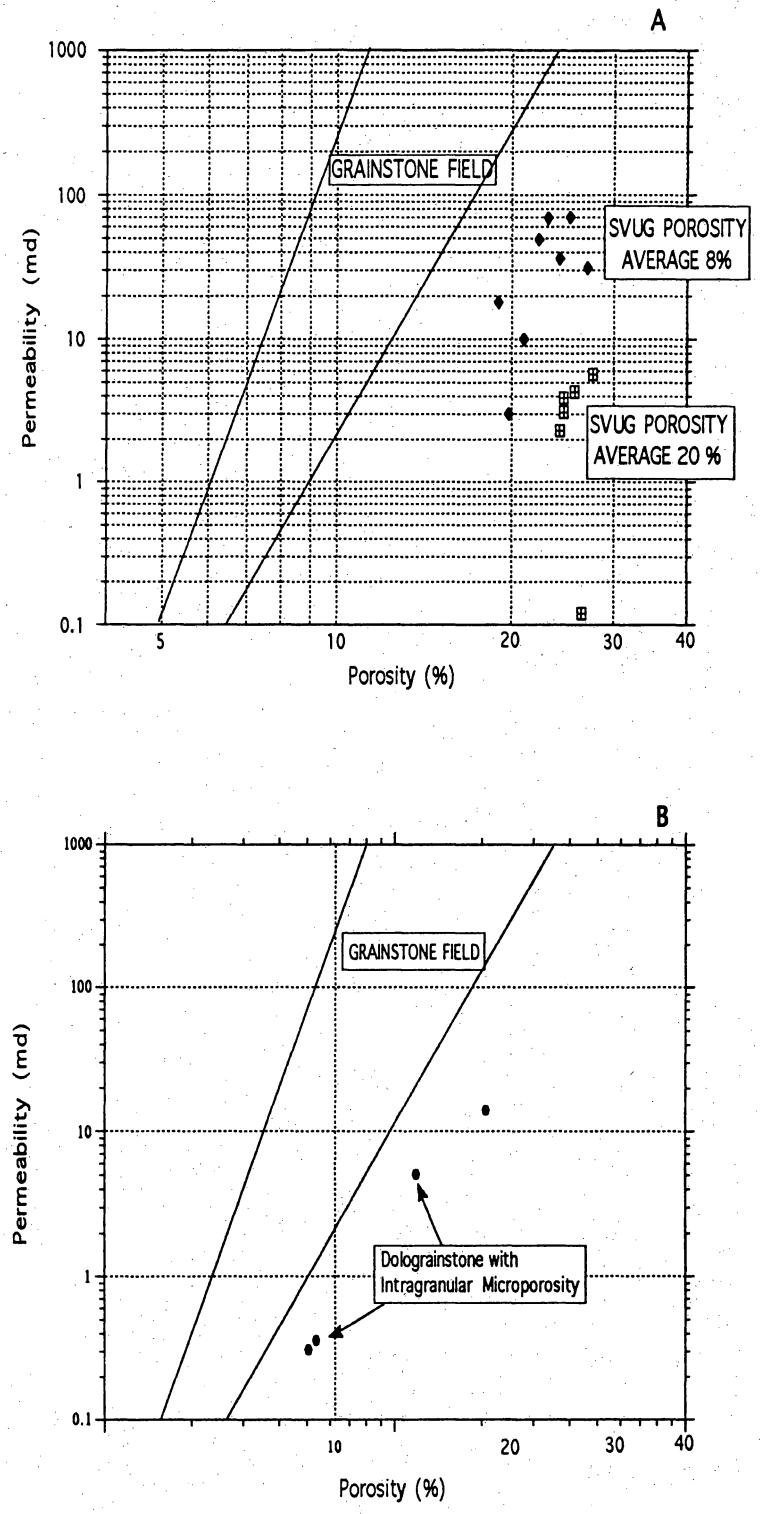

Figure 21. Cross plot illustrating the effect of separate-vug porosity on permeability. (A) Grainstones with separate-vug porosity in the form of grain molds plot to the right of the grainstone field in proportion to the volume of separate-vug porosity. (B) Dolograinstones with separate vugs in the form of intragranular microporosity plot to the right of the grainstone field.

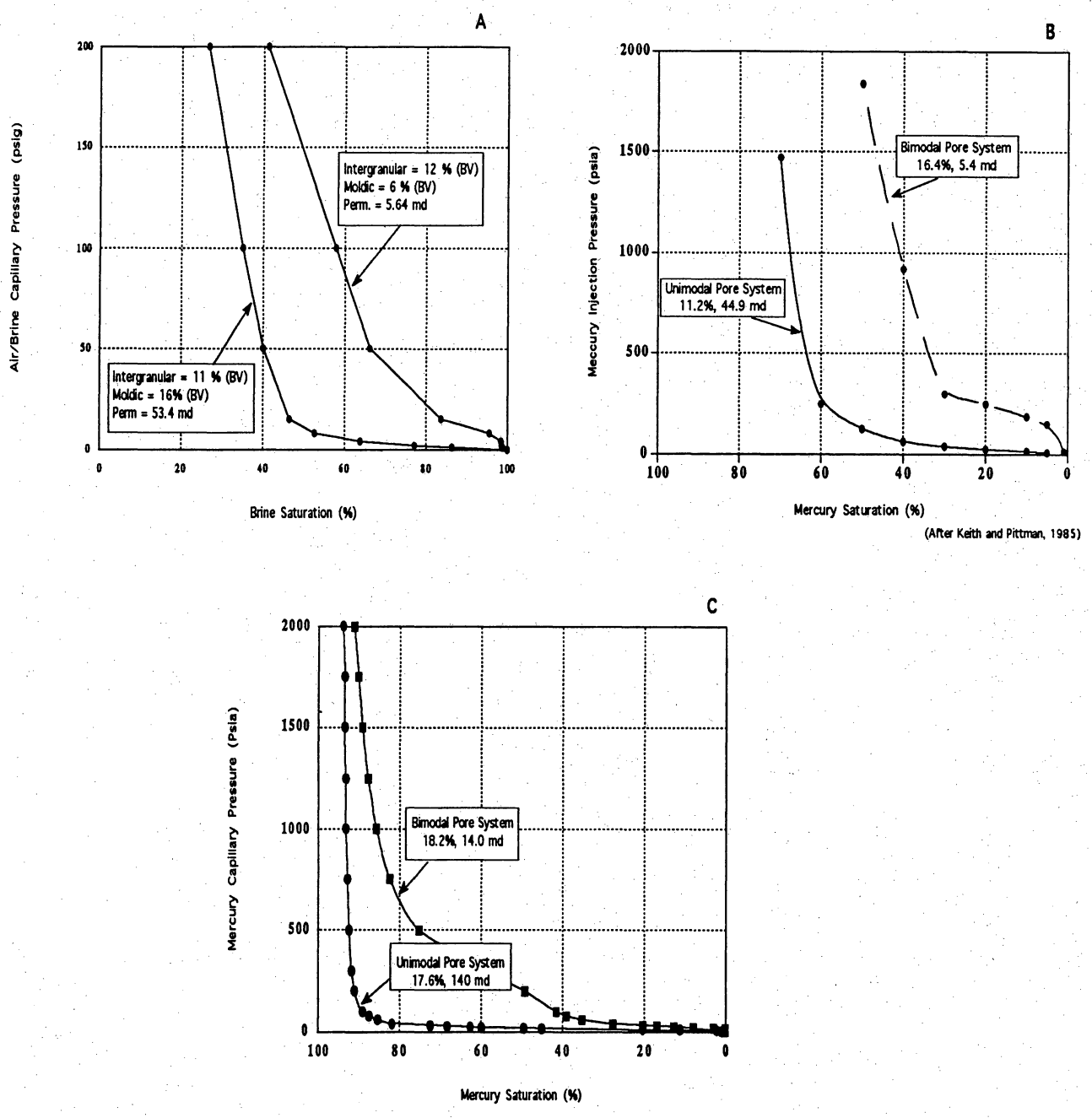

Figure 22. Capillary pressure curves illustrating the effect of moldic and intragranular-microporosity types of separate vugs on capillary properties. (A) Dolograinstones with large volumes of moldic porosity, San Andres Formation, Algerita Escarpment, New Mexico. (B) Oolid grainstone with intergranular porosity compared with ooid grainstone with both intergranular and intragranular-microporosity pore types, Rodessa limestone, Cretaceous, East Texas. (C) Dolograinstone with intergranular porosity compared with dolograinstone with both intergranular porosity and intragranular-microporosity pore types, Farmer San Andres field, West Texas.

Figure 23. Examples of touching-vug pore types. (A) Cavernous porosity in a Niagaran reef, Northern Michigan. (B) Collapse breccia, Ellenburger, West Texas. (C) Solution-enlarged fractures, Ellenburger, West Texas. (D) Cavernous porosity in Miami oolite, Florida. (E) Fenestral porosity in a pisolitic dolomite. Note that the pore space is more than twice the size of the enclosing grains.

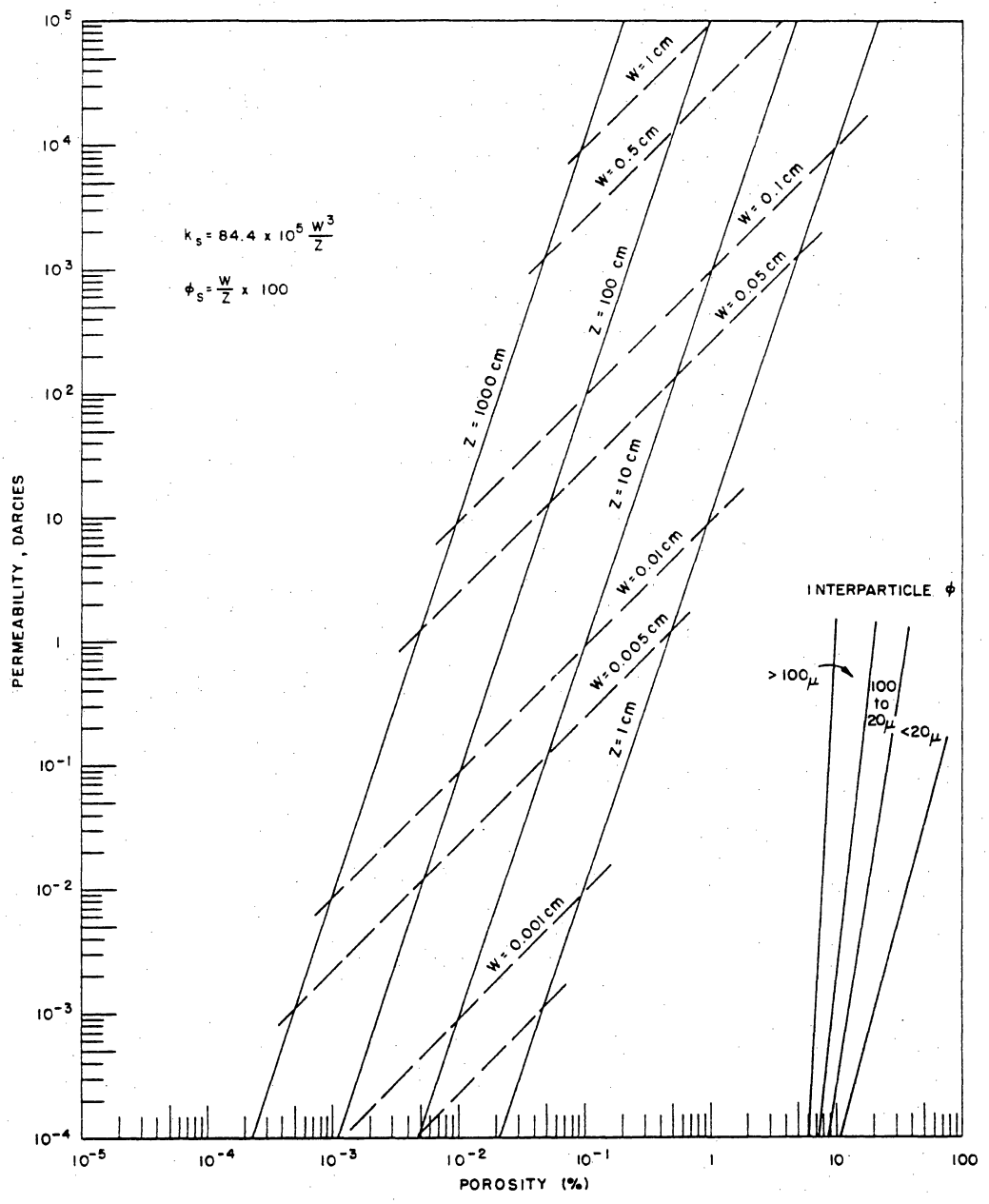

Figure 24. Theoretical fracture permeability-porosity relationship compared to the rock-fabric/petrophysical porosity, permeability fields (Lucia, 1983).

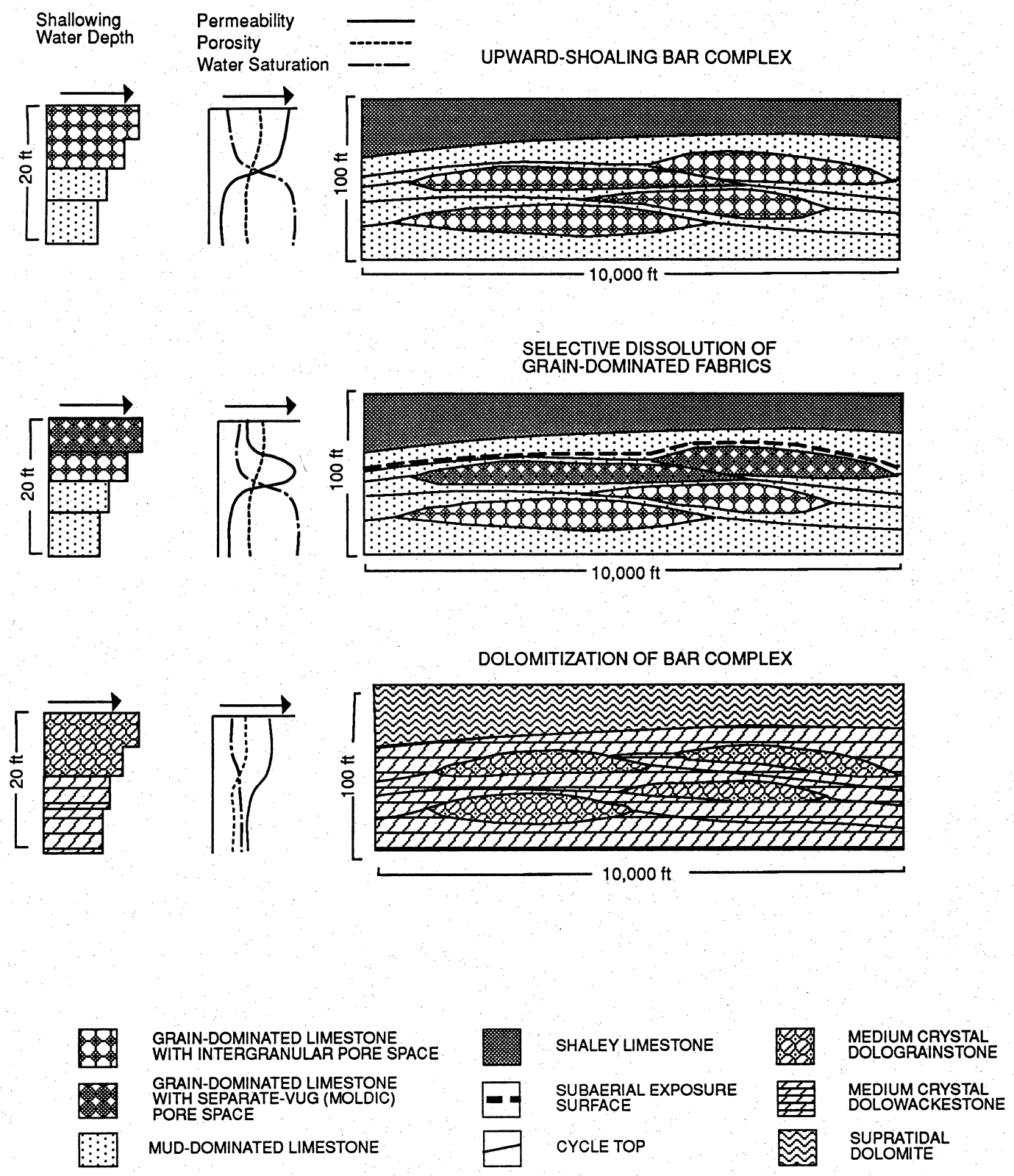

Figure 25. Examples of how the stacking of rock-fabric units affects the distribution of porosity, permeability, and water saturation in an upward-shoaling sequence with selective dissolution and dolomitization overprints.

Table 1. Values used to convert mercury/air capillary pressure to reservoir height.

Laboratory	**Reservoir**
(Mercury/air/solid)	(Oil/water/solid)
T = 480 dynes/cm	T = 28 dynes/cm
Ø = 140°	Ø = 44°
Water Density = 1.04	Oil Density = 0.88